JEE Journal of Ecological Engineering

Journal of Ecological Engineering, 2026, 27(2), 1–15
https://doi.org/10.12911/22998993/210597
ISSN 2299–8993, License CC-BY 4.0

Received: 2025.08.20
Accepted: 2025.12.15
Published: 2026.01.15

Evaluation and calibration of low-cost sensors for the measurement of $PM_{2.5}$, CO_2 and CO in urban contexts in the city of Milagro – Ecuador

Carlos A. Vaca Coronel[1*], Freddy L. Bravo Duarte[1], Delia D. Noriega Verdugo[1], Víctor H. Rea Sánchez[1], Javier A. Alcázar Espinoza[1]

[1] Universidad Estatal de Milagro, 091050, Ecuador
* Corresponding author's e-mail: cvacac3@unemi.edu.ec

ABSTRACT

Air pollution is a serious threat to public health worldwide, causing millions of premature deaths each year. In Latin America, and especially in Ecuador, the situation becomes even more complicated due to poor monitoring infrastructure, making it difficult to effectively track pollutants such as $PM_{2.5}$, CO_2 and CO. This research presents an innovative approach that is based on the calibration and validation of low-cost sensors (ME) to measure pollutants in outdoor spaces, using multivariate mathematical models (A, B, C and D) that include temperature and relative humidity as additional variables. Platforms with ME1 and ME2 sensors were used to collect the $PM_{2.5}$, CO_2 and CO data for more than two weeks, comparing these data with reference instruments. The calibration models were evaluated using metrics such as MAE, R^2, MAPE and SMAPE. The results indicated that, once calibrated, the ME1 and ME2 sensors achieved correlations above 92% with the reference instruments for all pollutants, with absolute and relative errors within acceptable ranges. The inclusion of environmental variables consistently improved the fit of the models, especially model D. Among the four approaches evaluated (A–D), Model D was the most efficient for $PM_{2.5}$, reaching $R^2 = 0.963$ and MAE = 3.24 µg/m³ in ME1 (8.5% improvement vs. Model A), and $R^2 = 0.957$ and MAE = 3.92 µg/m³ in ME2 (8.2% improvement). For CO_2, the differences between models were small (ME1: max. $R^2 = 0.839$ in D; ME2: max. $R^2 = 0.763$ in D), with MAE variations < 1%. For CO, the best performance was marginal and depended on the metric: in ME1, the lowest MAE was obtained by Model B (54.83 ppb), while in ME2, Model D (57.48 ppb) reduced the error by ~1.2% compared to A, with $R^2 \approx 0.929$. This study demonstrated that, with proper calibration, low-cost sensors can be effective tools for air quality monitoring in resource-limited contexts such as Ecuador, strengthening environmental surveillance strategies and facilitating evidence-based decision making.

Keywords: air quality, low-cost sensors, multivariate calibration models.

INTRODUCTION

Air quality is one of the most challenging global public health issues. According to the World Health Organization (WHO), air pollution is responsible for approximately seven million premature deaths per year, with fine particulate matter (PM2.5) and gases such as carbon dioxide (CO_2) and carbon monoxide (CO) being the main culprits (WHO, 2021). In Latin America, despite being less industrialized compared to other regions, there has been an increase in emissions in recent years due to urban growth, unregulated transportation and deficiencies in environmental monitoring. [1–3]. In middle- and low-income countries, such as Ecuador, the problem is exacerbated by limited infrastructure for continuous environmental monitoring. According to the data from the Ministry of Environment, Water and Ecological Transition (MAATE), the PM2.5 levels in urban areas, such as Quito and Guayaquil, have exceeded 25 µg/m³ on a daily average, a value that exceeds both the limits recommended by the WHO (15 µg/m³ per year) and the maximum permissible limits established in the country

(50 μg/m³ for PM2.5 in 24 hours according to MAATE Technical Standard No. 097-A). [4–7]

This research presents a proposal for the use, calibration and validation of low-cost sensors (LCS) for the measurement of air pollutants, using multivariable mathematical models that include corrections for temperature and relative humidity [8–11]. Unlike previous studies that only evaluated the linear correlation between sensors and reference equipment, this work incorporated four types of models (A, B, C and D) that allow evaluating the behavior of the sensors under changing environmental conditions and comparing them with quantitative criteria such as MAE, R^2, MAPE and SMAPE. [8, 12]

The importance of this research lies in its applicability for research work with limited resources, such as the Ecuadorian case, where air quality monitoring networks are scarce and costly to maintain. By demonstrating that inexpensive sensors can be adequately calibrated to fulfill indicative monitoring functions, an opportunity opens up to expand the coverage of environmental surveillance, contribute to compliance with national regulations and promote evidence-based public policies [10, 11]

Recent studies have delved into field calibration and statistical validation of low-cost sensors. For example, [13] showed how statistical correction in municipal networks reduces systematic biases at the neighborhood level; [14] evaluated calibration methods and reported modest but consistent improvements when environmental variables are incorporated; whereas [9] developed a multi-pollutant system and documented the usefulness of real-time multivariate approaches. The conducted work aligns with these findings by incorporating temperature and relative humidity into calibration models and advances by comparing four A–D formulations in parallel (with MAE, R^2, MAPE, and SMAPE metrics) and reporting the incremental benefit of environmental variables, especially for $PM_{2.5}$.

Methodology

This study focused on evaluating the performance of low-cost sensors (ME) for real-time monitoring of air pollutants, namely PM2.5, carbon dioxide (CO_2) and carbon monoxide (CO). A quantitative experimental design was used with a comparative approach between low-cost sensor readings and reference instruments. [15, 16]

The sensors selected were Sensor 0177 for PM2.5 and Sensor 0132 for CO and CO_2, [17–20]. They were chosen for their high availability, low cost and documented suitability for air quality monitoring applications. The sensors were integrated into platforms named ME1 and ME2 configured to record data at one-minute intervals. [13, 14, 21–23]. The 0177 sensor is an air quality sensor that uses a laser to measure the concentration of PM2.5 particles (fine particles with a diameter of 2.5 micrometers or less) in the air [24, 25]. This sensor provides accurate and real-time data on the amount of airborne particles in a range of 0.3 to 10 micrometers, the measurable particle diameter is 0.3~1.0, 1.0~2.5, and 2.5~10 micrometers. The 0132 sensor is designed to detect the concentration of CO and CO_2 in air, measuring concentrations between 20 to 2000 ppm, it offers an analog output interface, its sensitivity can be adjusted with an integrated potentiometer, as shown in Figure 1.

Study and site design

The study evaluated the calibration of low-cost sensors for $PM_{2.5}$, CO_2, and CO installed on two platforms (ME1 and ME2), compared against co-located reference stations. The campaign was conducted over 15 days in the city of Milagro, Ecuador, with variable weather conditions of temperature (T) and relative humidity (RH) representative of the period. Sensors ME1 and ME2 (Figure 2) were deployed together with reference instruments for at least 15 days in the center of the city of Milagro. Temperature (°C) and relative humidity (%) were also recorded simultaneously. The data were recorded in CSV format and processed in R (version 4.3.1) using the packages tidyverse, lubridate and ggplot2. Each platform recorded data every minute for 15 consecutive days, generating 21,600 records per variable and per platform. After cleaning (removal of negatives/duplicates, alignment by timestamp, and linear interpolation of short gaps), approximately 10.000 data points remained for ME1 and ME2 observations per pollutant. The analysis was performed on these synchronized and refined series.

Equipment and variables

- Sensors: ME1 and ME2 platforms with channels for $PM_{2.5}$, CO_2, and CO (gross ME output per channel).

Figure 1. Composition of sensors

Figure 2. Placement of sensors

- References: certified monitors for $PM_{2.5}$ ($\mu g \cdot m^{-3}$), CO_2 ($mg \cdot m^{-3}$), and CO (ppb).
- Environmental covariates: air temperature (T, °C) and relative humidity (RH, %) measured locally.

Data acquisition and preprocessing

- Sampling frequency: 1 min
- Synchronization: sensor and reference series were aligned by timestamp and interpolated or averaged to the common resolution of 5 min when necessary.
- Cleaning and quality control:
  - Elimination of duplicates and records with invalid dates.
  - Exclusion of physically impossible values such as negative values and values outside the range of the equipment [24–26].
- Sample size: number of observations per pollutant and platform after cleaning was approximately 10.000 data points for each pollutant

Negative or erroneous readings were filtered out and time stamps were aligned by linear interpolation to ensure comparability between time series. Duplicate and missing entries were removed, and outliers were detected using Tukey's method and Z-score analysis.

Calibration models

Four mathematical calibration models (A–D) were developed for each sensor based on previous research:

- Model A: Simple calibration using only the raw output of the ME1 or ME2 sensor.
- Model B: Multivariate calibration including temperature (T).
- Model C: Multivariate calibration including relative humidity (RH).
- Model D: Combined multivariate calibration using ME, T and RH.

The general forms of the models were:

- Model A: $y = \beta_0 + \beta_1.ME$
- Model B: $y = \beta_0 + \beta_1\text{-}ME + \beta_2.T$
- Model C: $y = \beta_0 + \beta_1\text{-}ME + \beta_2.RH$
- Model D: $y = \beta_0 + \beta_1.ME + \beta_2.T + \beta_3.RH$.
- donde "*y*" es la concentración de la referencia, ME la lectura del sensor.

Performance metrics calculated for each model included mean absolute error (MAE), coefficient of determination (R^2), mean absolute percentage error (MAPE) and symmetric MAPE (SMAPE). They were calculated separately for ME1 and ME2 and compared between models. Statistical analysis and visualization were performed in R. Scatter plots and time series were created with ggplot2; correlations were evaluated

with ggcorrplot, and regression fits were visualized with geom_smooth(method = "lm"). Five-fold cross-validation was applied to ensure robustness of model comparisons. [27–30]. To formally compare the performance of the four models (A–D), k=5 cross-validation was applied by time blocks. In each fold, the model was trained on the four time quintiles and evaluated on the remaining quintile.

A repeated measures ANOVA was performed on the metrics per fold (MAE and R^2) with fold as a block (Error(fold)) and Model (A–D) as a fixed factor. Additionally, a linear mixed model with random intercept per fold was fitted for more robust contrasts, and Tukey post hoc comparisons (multiplicity adjustment) were performed between pairs of models. As a sensitivity analysis, paired Student's t-tests were calculated between pairs of models per fold. For visualization, the scatter plots include the 95% confidence band of the linear fit, and for model D, a 95% prediction interval is reported at the median temperature and humidity of the evaluated set.

ANALYSIS OF RESULTS

Analysis of $PM_{2.5}$

The relative humidity graph (Figure 3), shows the behavior over time of $PM_{2.5}$ captured by the low-cost sensors (ME1 and ME2) compared to the reference instrument, along with the evolution of relative humidity (RH). It is observed that both sensors manage to adequately replicate the $PM_{2.5}$ concentration trends, although they present slight variations in the high concentration peaks. RH evidences a daily variability, without a very marked direct relationship with $PM_{2.5}$ levels. The temperature graph (Figure 4) presents the

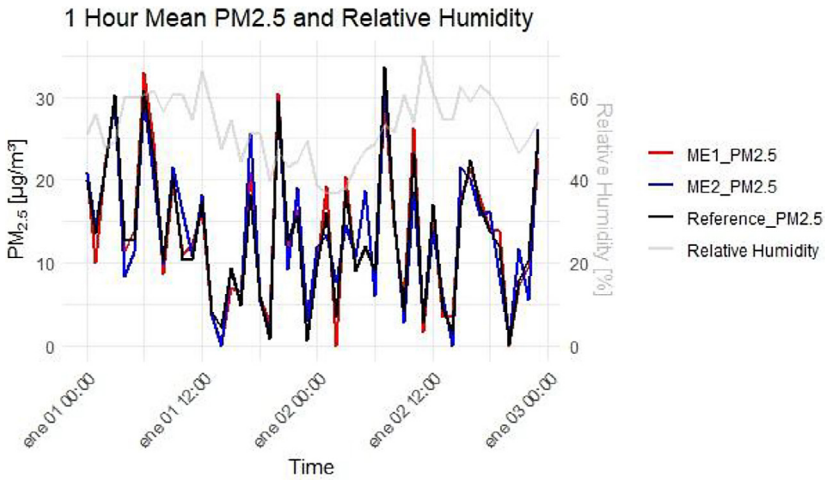

Figure 3. Relative humidity and PM2.5

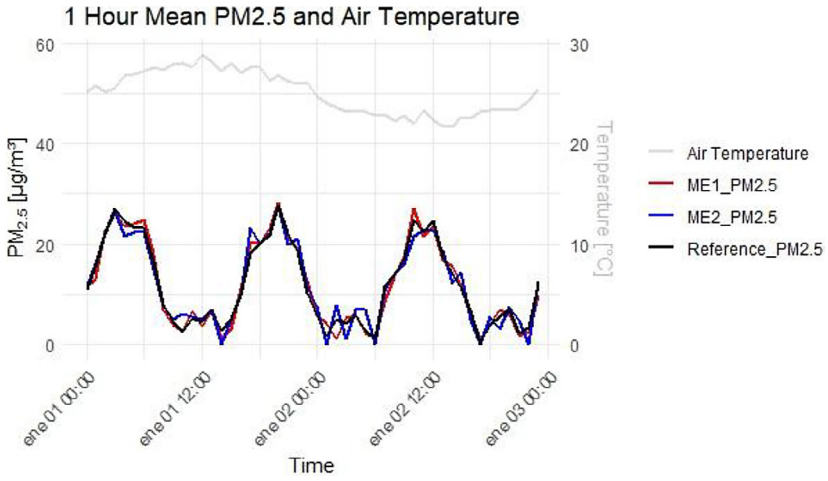

Figure 4. Temperature and PM2.5

comparison of $PM_{2.5}$ It was identified that both ME1 and ME2 follow in a very similar way the trend of the reference, particularly in the daily rises and falls, while temperature remains more stable, suggesting a lower direct influence of this variable on $PM_{2.5}$ concentrations in this measurement period.

The correlation matrix (Figure 5) demonstrates the obtained findings, showing high correlation coefficients between the ME1 and ME2 sensors with respect to the reference instrument (0.98 and 0.94, respectively), which evidences a strong linear relationship and a good ability to reproduce the real $PM_{2.5}$ values. The correlation between RH and $PM_{2.5}$ measurements is low

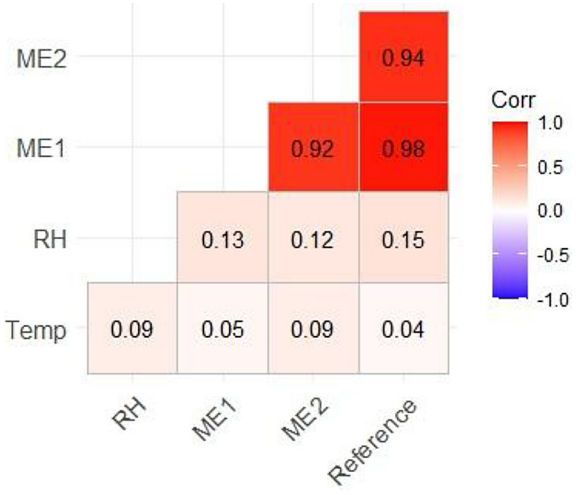

Figure 5. PM2.5 correlation

(between 0.12 and 0.15), indicating that relative humidity did not significantly affect the measurement during the experiment. Likewise, temperature shows even lower correlations (between 0.04 and 0.09), confirming its low influence in the analyzed period.

Figure 6 presents the relationship between the $PM_{2.5}$ concentrations measured by the low-cost sensors (ME1 and ME2) and the reference measurements, both before and after the calibration process. In the first graph ("ME1 vs Reference (Uncorrected)"), it can be seen that the ME1 sensor, without correction, shows a reasonably strong linear trend with the reference, albeit with some scatter in the data, particularly at concentrations greater than 20 µg/m³.

After calibration ("ME1 vs Reference (Corrected)"), the scatter decreases markedly and the points align much more closely along the line of identity (dashed line), indicating a significant improvement in the accuracy of the sensor. This result suggests that the fitting model applied to ME1 was highly effective. Similarly, the ME2 sensor ("ME2 vs Reference (Uncorrected)") also exhibits a positive correlation before correction, but with greater data variability relative to ME1, especially at the upper extremes of concentration. After calibration ("ME2 vs Reference (Corrected)"), the ME2 data improves in alignment, although the fit is not as perfect as in the case of ME1, indicating that the corrective model had a

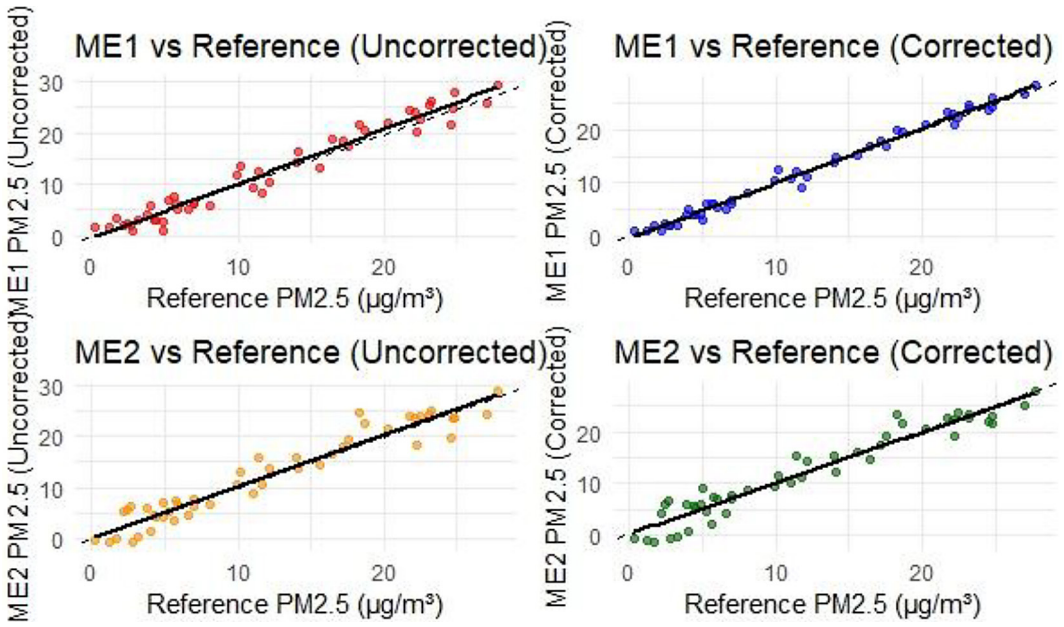

Figure 6. PM2.5 concentration

positive impact, but that there is still room for improvement for the ME2 sensor.

The results obtained from the calibration models for the ME1 and ME2 sensors show a considerable improvement in accuracy and precision after multivariate adjustment. In the case of the ME1 sensor, the simplest model (Model A) presents a coefficient of determination $R^2 = 0.951$ and a MAE of 3.54 μg/m³, indicating a strong but still perfectible relationship with respect to the reference values. By introducing additional variables, such as temperature (T) in Model B and relative humidity (RH) in Model C, a progressive improvement in the metrics is observed. Model D, which simultaneously integrates T and RH, achieves the best performance with $R^2 = 0.963$, MAE = 3.24 μg/m³, MAPE = 14.96% and SMAPE = 13.75%, evidencing that multivariate calibration is highly effective in improving the response of the ME1 sensor.

For the ME2 sensor, a similar pattern is observed, although with slightly lower values than ME1. The initial model (Model A) starts with $R^2 = 0.944$ and MAE = 4.27 μg/m³. The incorporation of T in Model B and RH in Model C improves the metrics, highlighting Model D, which integrates both variables and achieves an R^2 of 0.957, a MAE of 3.92 μg/m³, a MAPE of 17.33% and a SMAPE of 15.66%. Despite the improvements, the relative errors (MAPE and SMAPE) are higher in ME2 than in ME1, suggesting that the ME2 sensor has greater inherent variability or sensitivity to unmodeled environmental conditions.

For both sensors, it is highlighted that the addition of temperature and humidity as independent variables in the regression models consistently improves the fit. This evidences the importance of considering environmental factors in the calibration of low-cost sensors for $PM_{2.5}$ measurements. Also, the SMAPE values obtained, which remain around 14–16%, indicate an acceptable relative error for environmental monitoring applications of an indicative type or in support of official networks (Table 1, 2).

Figure 7 shows the temporal evolution of CO_2 concentrations measured by sensors ME1 and ME2 compared to a reference instrument, together with the evolution of the environmental variables of relative humidity (RH) and temperature (Figure 8). It is observed that both sensors, although following the general trends of the reference, present variations in magnitude throughout the measurement period. The ME1 sensor tends to slightly overestimate the CO_2 values with respect to the reference, while the ME2 sensor shows a more marked underestimation, as evidenced in the humidity and temperature plots.

The impact of environmental conditions is reflected in the observed correlations. The correlation matrix shows that ME1 has a correlation of 0.92 with the reference value, while ME2 reaches 0.93, suggesting a high capacity of both sensors to capture CO_2 variability, although with systematic differences in magnitude. However, the correlation levels of the sensors with RH and temperature are low (around 0.08 to 0.2), indicating that, despite the influence of these variables, their effect is not dominant in the range of variability studied (Figure 9).

The trend of relative humidity shows smoother variations than those of CO_2, while temperature, although less variable, presents certain peaks that coincide with fluctuations in CO_2 concentration, suggesting an indirect interaction. This environmental influence should be considered in advanced calibrations to improve accuracy.

Table 1. Calibration of low-cost PM2.5 sensors

Model	Equation	MAE (μg/m³)	R^2	MAPE (%)	SMAPE (%)
ME1					
A	$y = 0.902 * ME1_{PM2.5} + 0.999$	3.54	0.951	16.21	14.91
B	$y = 0.114 + 0.901ME1_{PM2.5} + 0.036T$	3.27	0.962	15.02	13.80
C	$y = 0.116 + 0.9ME1_{PM2.5} + 0.017RH$	3.49	0.953	15.98	14.71
D	$y = -0.601 + 0.899ME1_{PM2.5} + 0.03T + 0.016RH$	3.24	0.963	14.96	13.75
ME2					
A	$y = 0.922ME2_{PM2.5} + 0.678$	4.27	0.944	18.78	16.99
B	$y = 0.617 + 0.992ME2_{PM2.5} + 0.002T$	3.96	0.956	17.47	15.79
C	$y = 0.141 + 0.921ME2_{PM2.5} + 0.01RH$	4.23	0.947	18.55	16.76
D	$y = 0.16 + 0.921ME2_{PM2.5} - 0.001T + 0.011RH$	3.92	0.957	17.33	15.66

Table 2. PM2.5 calibration models (ME1/ME2): Cross-validated performance (MAE, R^2) and Improvement vs. baseline (A)

PM2.5
ME1: better D (MAE = 3.24 µg/m³; R^2 = 0.963); improvement vs. A = 8.47% in MAE
ME2: better D (MAE = 3.92 µg/m³; R^2 = 0.957); improvement vs. A = 8.20% in MAE

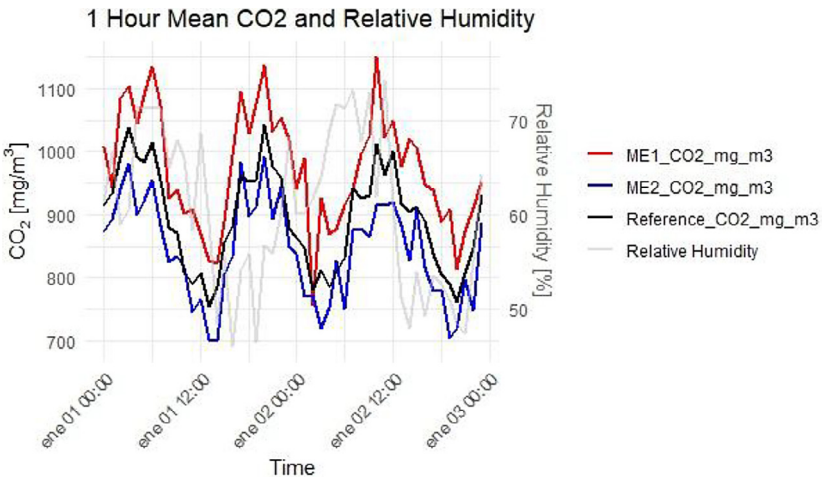

Figure 7. Relative humidity in the measurement of CO_2

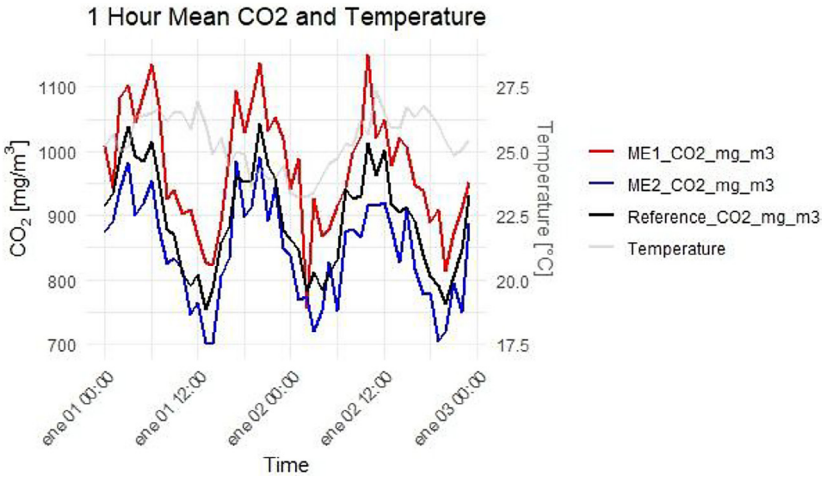

Figure 8. Temperature in CO_2 measurement

Figure 10 compares the carbon dioxide (CO_2) concentration measurements obtained by the ME1 and ME2 sensors versus the reference instrument, both in their raw state (Raw) and after adjustment (Adjusted). In the Raw data plots, it is observed that the measurements of both sensors present a larger scatter around the identity line (dashed line), particularly ME2, indicating significant biases and systematic errors before any calibration process.

After applying the fit models, the Adjusted plots show a marked improvement in the alignment of the data with respect to the reference. For

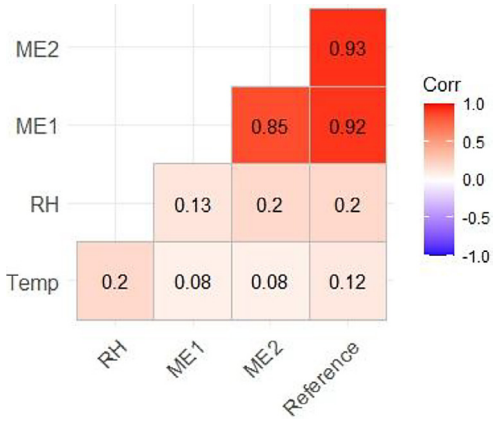

Figure 9. CO_2 correlation

ME1, calibration reduces the scatter and brings the data significantly closer to the ideal line, reflecting a successful fit. For ME2, although the calibration improves the trends, a slight scatter remains, indicating that, although the model corrects the overall trend, residual errors – that could be optimized with more complex techniques or with the inclusion of additional environmental variables – still persist.

In terms of interpretation, the fit has systematically reduced the prediction errors for both sensors, as can be deduced from the slope of the regressions, which is closer to 1, and the intersections closer to 0. In addition, the smaller separation between the fitted regression line and the identity line in the corrected plots suggests a high ability of the sensors to reproduce CO_2 levels once calibrated.

The calibration of the ME1 and ME2 sensors against CO_2 reference measurements shows differentiated performances according to the mathematical model used. For ME1, all models (A-D) present a low mean absolute error (MAE), close to 26.3 mg/m³, and a coefficient of determination (R^2) higher than 0.83, indicating a good fit of the predictions to the reference values. The inclusion of environmental variables, such as temperature (T) and relative humidity (RH) slightly improves the R^2, reaching a maximum value of 0.839 in Model D.

Regarding the relative errors, the MAPE for ME1 remains around 2.97–2.98%, while SMAPE, a robust indicator in the face of extreme values, is consistently around 2.93–2.94%. These low values suggest high prediction accuracy and confirm that the calibrations performed are effective for environmental applications requiring high accuracy.

In the case of the ME2 sensor, the errors are slightly higher. The MAE oscillates around 31.5 mg/m³, and the R^2 is somewhat lower, in the range of 0.759–0.763. Although the models that include temperature and humidity (Models B–D) achieve small improvements in R^2, the increase is not as pronounced as in ME1, indicating that ME2 has greater linearity or intrinsic stability limitations. The MAPE and SMAPE for ME2 remain low (3.58–3.61% and 3.52–3.55%, respectively), but higher than those obtained for ME1, reflecting slightly lower performance.

Overall, the results show that the ME1 sensors offer a more robust and reliable response compared to ME2. In addition, the incorporation of auxiliary meteorological variables such as temperature and humidity improves the performance of both sensors, although more significantly in ME1. The choice of the calibration model should consider not only the values of R^2, MAE and MAPE, but also the operational stability of the sensor under varying environmental conditions. See Table 3, 4.

In the temporal behavior plots (Figures 11 and 12), it is observed that the scaled signals from the ME1 and ME2 carbon monoxide (CO) sensors reasonably replicate the trends of the reference, albeit with differences in magnitude. The CO Reference_ppb values exhibit pronounced

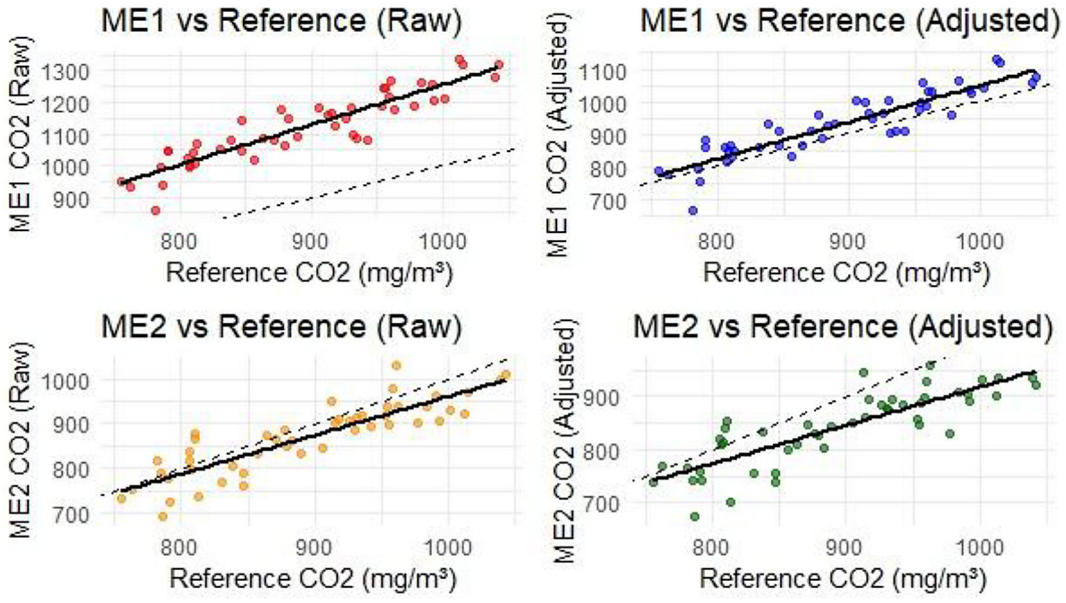

Figure 10. Measurement of the CO_2 concentration

Table 3. Calibration of the CO_2 sensors

Model	Equation	MAE (mg/m³)	R^2	MAPE (%)	SMAPE (%)
ME1					
A	$y = 0.65 * ME1_{co2} + 159.53$	26.30	0.831	2.97	2.93
B	$y = 86.58 + 0.65ME1_{co2} + 2.98T$	26.29	0.832	2.97	2.93
C	$y = 117.90 + 0.65ME1_{co2} + 0.84RH$	26.30	0.838	2.97	2.93
D	$y = 74.98 + 0.65ME1_{co2} + 1.85T + 0.79RH$	26.37	0.839	2.98	2.94
ME2					
A	$y = 0.88ME2_{co2} + 131.81$	31.74	0.759	3.61	3.55
B	$y = 25.88 + 0.87ME2_{co2} + 4.31T$	31.58	0.762	3.59	3.53
C	$y = 118.31 + 0.87ME2_{co2} + 0.32RH$	31.48	0.760	3.58	3.52
D	$y = 24.17 + 0.87ME2_{co2} + 4T + 0.22RH$	31.58	0.763	3.60	3.54

Table 4. CO_2 calibration models (ME1/ME2): Cross-validated performance (MAE, R^2) and Improvement vs. baseline (A)

CO_2
ME1: better than B (MAE = 26.29 mg/m³; max. R^2 with D = 0.839); improvement vs. A = 0.04% in MAE (marginal).
ME2: better than C (MAE = 31.48 mg/m³; max. R^2 with D = 0.763); improvement vs. A = 0.82% in MAE (marginal)

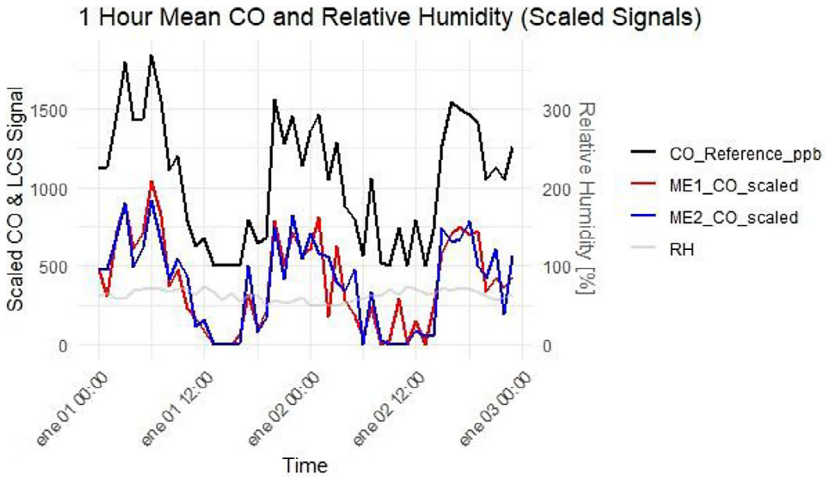

Figure 11. Relative humidity and CO

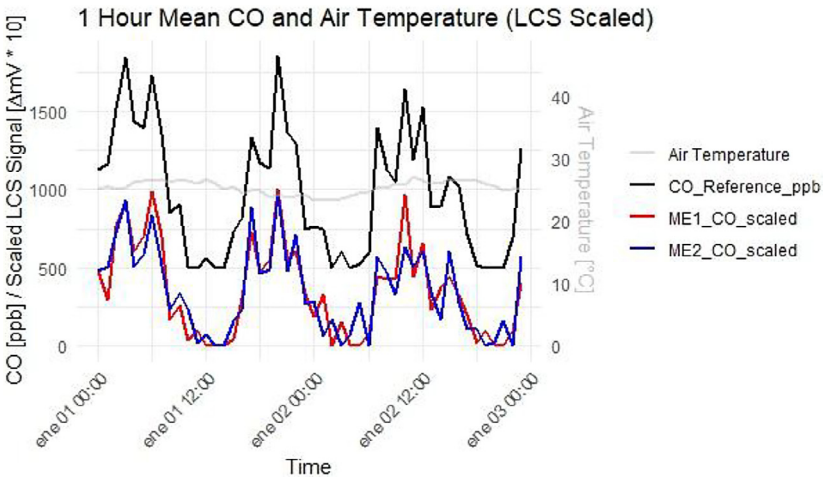

Figure 12. Temperature at CO

peaks that are also partially captured by ME1 and ME2, but with obvious attenuation in the signals from the low-cost sensors. This discrepancy suggests limitations in the sensitivity of ME sensors to abrupt changes in CO concentration.

Regarding the environmental variables, relative humidity (RH) shows a constant trend during the measurement, with slight fluctuations that do not seem to significantly affect the response of the sensors, given the low level of correlation observed afterwards. On the other hand, temperature shows a moderate variation between 15 °C and 35 °C, and its stable behavior could explain the reduced effect of this parameter on the dispersion of the signals.

The correlation matrix (Figure 13) reinforces these findings: both ME1 and ME2 exhibit a strong correlation with the reference (R^2 of 0.92 and 0.93, respectively), evidencing a good overall tracking capability of environmental CO trends. However, the correlations between sensors and meteorological variables (RH and Temp) are low (between 0.08 and 0.20), suggesting that, in this data set, environmental conditions do not significantly affect the direct measurement of CO.

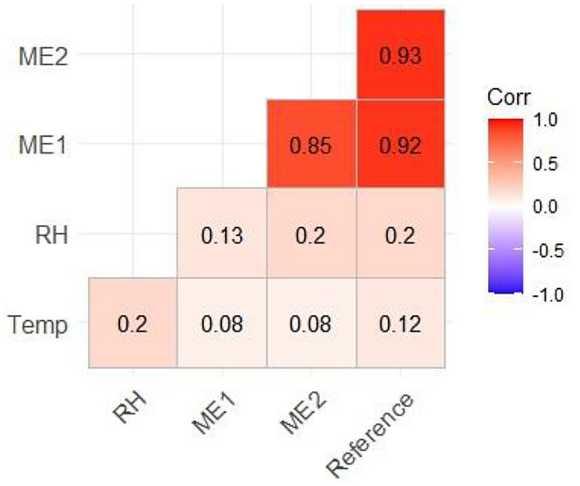

Figure 13. CO correlation matrix

These results are relevant as they indicate that, although there is good overall monitoring of CO concentrations, additional calibrations or correction models should consider the limited response of the sensors to sharp peaks, particularly under the conditions of high environmental variability. Similarly, the high correlation between ME1, ME2 and the reference validates the potential of these devices for low-cost urban monitoring applications, although caution should be exercised in the situations where maximum accuracy is required at extreme values. Figure 14 presents the comparison between the CO concentrations measured by the ME1 and ME2 sensors, in their raw and adjusted states, with respect to a high precision reference. The scatter plots show that, for both sensors, there is a positive linear relationship between the sensor measurements and the reference, indicating a basic ability to track variations in CO levels.

In the raw plots, both ME1 and ME2 tend to slightly overestimate CO concentrations compared to the reference, with several points lying above the identity line (dashed line). This systematic deviation suggests the need to apply correction models to improve the accuracy of the measurements.

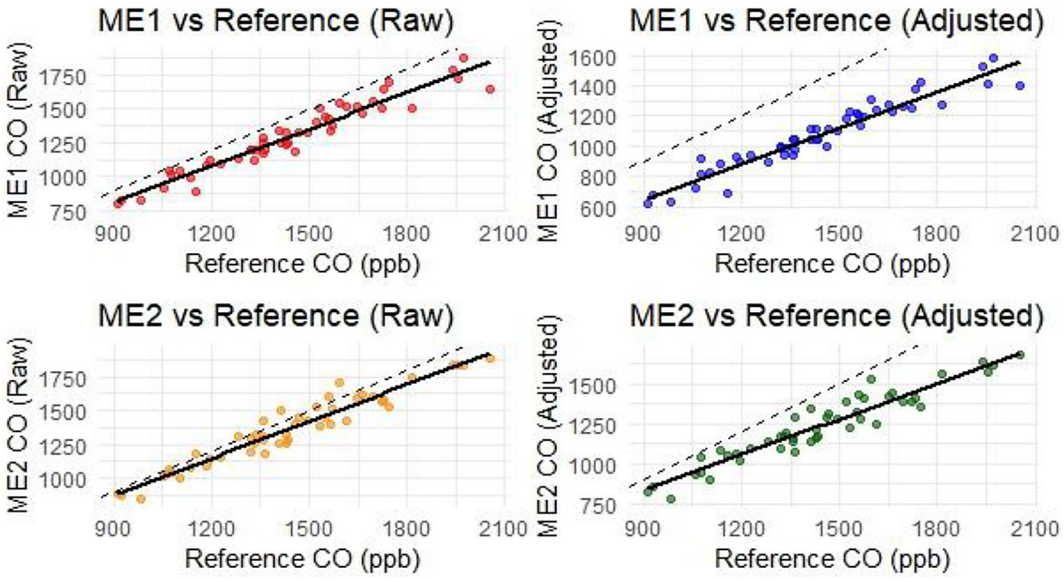

Figure 14. Measurement of CO

After correction (Adjusted), the data dispersions on both sensors show better alignment with the reference. Especially in ME2, the point cloud is closer to the identity line, indicating an improvement in accuracy and reduction of systematic bias. However, slight scattering is still observed, particularly at higher CO concentration levels, which could be related to intrinsic limitations in the response range of the sensors.

Comparatively, the ME2 sensor seems to benefit more from the applied adjustment, presenting a more homogeneous distribution and lower error with respect to the reference. On the other hand, ME1, although it improves substantially after the correction, still presents some values far from the line of equality, especially at high concentrations.

In conclusion, the implemented calibration clearly improves the quality of CO measurements for both sensors, bringing them closer to the expected behavior with respect to the reference. However, there are still slight differences that should be considered, if these devices are used in highly demanding applications, such as regulatory environmental monitoring or epidemiological investigations.

Table 5 presents the performance of four calibration models (Models A, B, C and D) for the ME1 and ME2 sensors in relation to a reference measurement of carbon monoxide (CO) in parts per billion (ppb). The following metrics were evaluated: MAE, R^2, MAPE (%) and SMAPE (%).

For ME1, all models present a coefficient of determination $R^2 \approx 0.928–0.929$, which evidences a very good explanatory capacity of the model, with very little difference between considering or not the adjustment variables (Temperature and Relative Humidity). MAE ranges between 54.83 and 55.50 ppb, with Model B (with temperature as an auxiliary variable) achieving the lowest mean absolute error. In addition, SMAPE remains low in all models, between 3.79% and 3.85%, indicating a very good symmetry in the relative errors.

For ME2, the results are similar, with R^2 also close to 0.928–0.929, showing that the predictions are highly consistent. MAE is slightly higher with respect to ME1 (57.48 to 58.20 ppb), suggesting that ME2 has slightly higher errors. The SMAPE values for ME2 are between 4.02% and 4.07%, very competitive for this type of low-cost sensor, although slightly higher than those of ME1.

As for the models, for both sensors, Models B and D tend to marginally improve the errors with respect to the base model A, owing to the incorporation of temperature and humidity. Model D (with T and RH) shows the lowest MAPE and SMAPE for ME2 (17.33% MAPE and 4.02% SMAPE), suggesting that including both environmental variables improves the prediction slightly, but consistently (Table 6).

The scatter plots in Figure 15 show the sensor–reference relationship for each pollutant ($PM_{2.5}$, CO_2, and CO) and platform (ME1 and ME2). The linear regression line (OLS) and its 95% confidence band are superimposed on the observed points, quantifying the uncertainty of the estimated mean of the response (reference) conditioned on the predictor (sensor reading). Visually, the slope and intercept provide information on scale bias (slope other than 1) and additive bias (intercept other than 0), while the dispersion of the points around the line reflects the residual calibration error. The width of the band narrows around the region with the most observations and widens at the extremes (greater leverage), which is to be expected in linear models.

Together, these figures allow: (i) confirming whether the calibration captures the central trend

Table 5. Calibration in the measurement of CO

Model	Equation	MAE (ppb)	R^2	MAPE (%)	SMAPE (%)
ME1					
A		55.07	0.928	16.21	3.80
B	$y = -11.58 + 1.03ME1_{co} + 4.67T$	54.83	0.928	15.02	3.79
C	$y = 51.14 + 1.03ME1_{co} + 0.92RH$	55.02	0.929	15.98	3.81
D	$y = 450.10 + 1.02ME1_{co} - 23.90T + 4.29RH$	55.50	0.929	14.96	3.85
ME2					
A	$y = 1.01ME2_{co} + 59.16$	58.20	0.928	18.78	4.07
B	$y = -124.82 + 1.01ME2_{co} + 7.39T$	57.64	0.928	17.47	4.03
C	$y = 16.60 + 1.01ME2_{co} + 0.74RH$	57.94	0.928	18.55	4.05
D	$y = -672.92 + 1.02ME2_{co} + 41.13T - 5.06RH$	57.48	0.929	17.33	4.02

Table 6. CO calibration models (ME1/ME2): Cross-validated performance (MAE, R^2) and Improvement vs. baseline (A)

CO
CO — ME1: better than B (MAE = 54.83 ppb; $R^2 \approx 0.928–0.929$); improvement vs. A = 0.44% in MAE (marginal)
CO — ME2: better than D (MAE = 57.48 ppb; $R^2 \approx 0.929$); improvement vs. A = 1.24% in MAE (marginal).

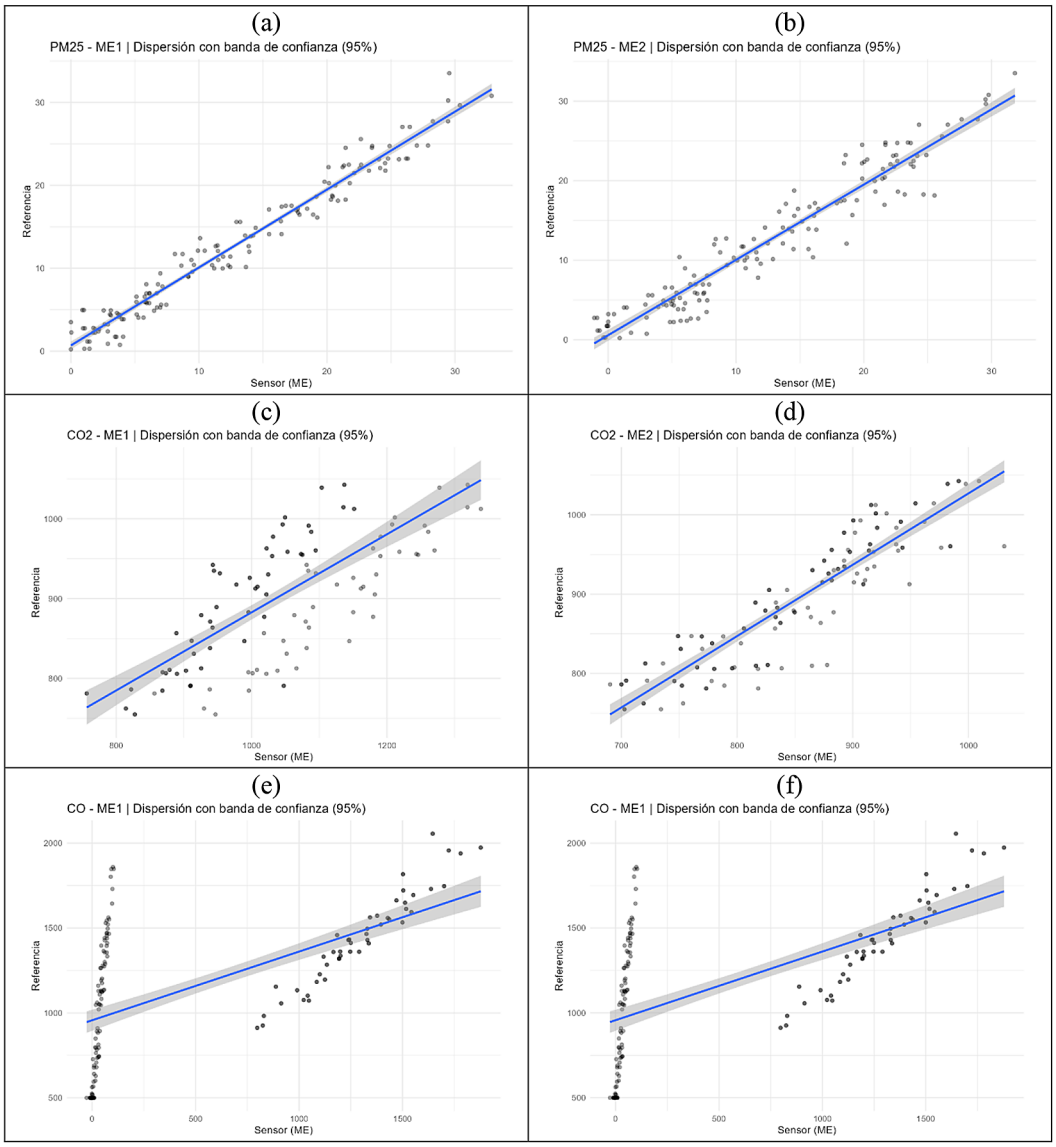

Figure 15. Sensor vs. reference scatter plots with 95% confidence band for the six cases ($PM_{2.5}$ and CO_2 and CO; ME1 and ME2 platforms). Points: observations; line: OLS fit; shading: 95% confidence band of the fit

between the sensor and the reference, (ii) identifying the possible non-linearities or saturation zones (e.g., curvatures or range of residuals at high concentrations), and (iii) comparing, for the same pollutant, the relative performance of ME1 vs. ME2: a more compact cloud and a narrower confidence band suggest greater model stability. The visual interpretation is complemented by statistical analyses (ANOVA), which verify whether the differences in performance between models A–D are significant. Figure 16. For the cases where temperature (T) and relative humidity (RH) are measured simultaneously, Model D (ME + T + RH) and its 95% prediction interval are presented, setting T and RH at their medians to isolate the effect of the sensor signal (ME). Unlike the confidence band, which describes the uncertainty about the mean of the response, the prediction interval

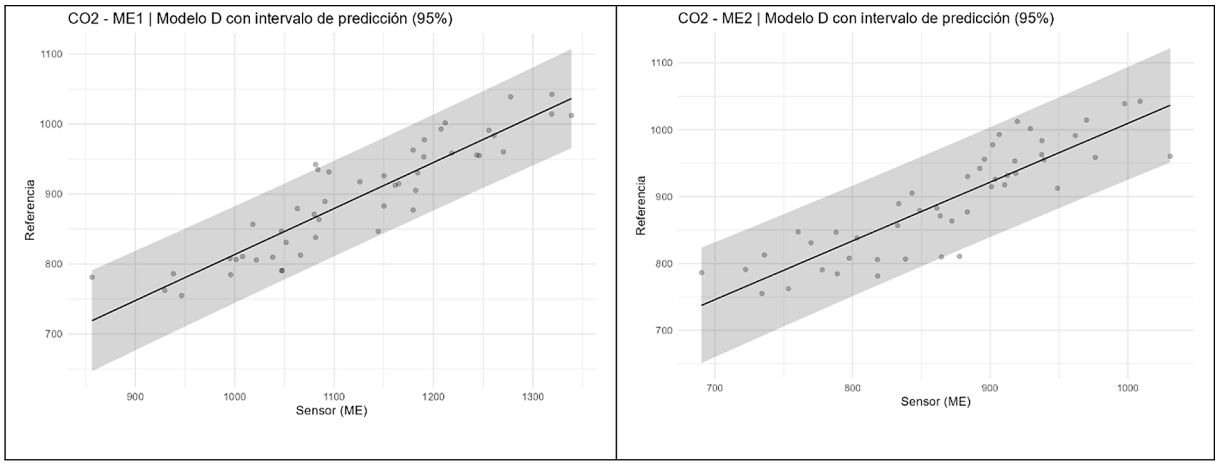

Figure 16. 95% prediction interval for Model D (ME, T, and RH) with T and RH fixed at their medians. Line: prediction; shading: 95% prediction interval, reflecting the expected variability of new observations (wider than the confidence band)

also incorporates the residual variability of future observations; therefore, it is wider and represents the total prediction uncertainty for new data. This visualization allows the practical usefulness of the calibration to be evaluated: a narrow prediction band suggests that, given ME, T, and RH, future reference observations will fall within a narrow range (better predictive capacity). Likewise, when comparing platforms, a systematic shift in the curve or a greater amplitude of the interval indicates greater unexplained error or residual sensitivity to T/RH. The consistency between these figures and the ANOVA/Tukey results supports when the joint inclusion of T and RH provides real gains in accuracy over simpler models.

As it can be seen in Table 7, the analysis of variance with repeated measures revealed overall differences between models in five of the six contaminant-platform combinations. For CO, significant differences were observed in both ME1 ($F(3,8)=76.31$, $p=6.16\times10^{-6}$) and ME2 ($F(3,8)=26.44$, $p=0.000298$); in both cases, the best performance corresponded to C (ME+RH), with 77.61±11.96 ppb in ME1 and 138.09±28.64 ppb in ME2. For CO_2, there were also overall differences (ME1: $F(3,12)=25.56$, $p=1.69\times10^{-5}$; ME2: $F(3,12)=18.7$, $p=8.09\times10^{-5}$), but the winning model was platform-dependent: in ME1, D (ME+T+RH) prevailed with 29.42±6.14, while in ME2, the lowest MAE was obtained by A (ME) with 28.70±5.35. In $PM_{2.5}$, the effect was uneven: in ME1, no differences were detected between models ($F(3,8)=0.447$, $p=0.654$) and, for parsimony, the best average was A (ME) with 1.31±0.24 µg/m³; in ME2 there were differences ($F(3,8)=6.565$, $p=0.0205$) and B (ME+T) was superior with 1.79±0.32 µg/m³. Overall, the results confirm that the inclusion of environmental covariates can reduce calibration error, although their benefit is specific to the pollutant.

DISCUSSION

The results show that the comparison between A–D calibration models is not uniform across contaminants or platforms. For CO, ANOVA detected overall differences in ME1 and ME2

Table 7. ANOVA statistical comparison

Contaminante	Plataforma	ANOVA	p	Mejor modelo (MAE_ mean ± DE)
CO	ME1	F(3.8) = 76.31	6.16e-06	C (77.61 ± 11.96)
CO	ME2	F(3.8) = 26.44	0.000298	C (138.09 ± 28.64)
CO2	ME1	F(3.12) = 25.56	1.69e-05	D (29.42 ± 6.14)
CO2	ME2	F(3.12) = 18.7	8.09e-05	A (28.70 ± 5.35)
PM25	ME1	F(3.8) = 0.447	0.654	A (1.31 ± 0.24)
PM25	ME2	F(3.8) = 6.565	0.0205	B (1.79 ± 0.32)

($p \ll 0.001$), and Model C (ME+RH) performed best; this suggests cross-sensitivity to humidity in electrochemical CO measurement and supports the inclusion of RH as a corrective covariate. For CO_2, there were significant differences, but the winning model depended on the sensor: in ME1, Model D (ME+T+RH) obtained the lowest MAE, while in ME2, A (ME only) was sufficient, pointing to different designs/firmware or thermal response between platforms; adding T and RH does not always help when the electronics already partially compensate for these effects. In $PM_{2.5}$, ME1 showed no significant differences between models, indicating that the base form (A) captures variability well; in ME2, B (ME+T) outperformed the others, probably because air density/temperature slightly influences the optical response of the ME2 channel. These conclusions are supported by the reported fit statistics (MAE and R^2) and by the ANOVA by pollutant/platform, which identifies the model with the lowest average error.

From a practical perspective, the benefit of adding covariates was moderate for $PM_{2.5}$ and CO_2 and clearer for CO; therefore, specific model selection is recommended for each pollutant and platform: D or B should be used when RH/T provide systematic error reduction, and A should be retained when the gain is marginal (avoiding overfitting and unnecessary complexity). The 95% confidence bands in the scatter plots visually confirm the consistency of the fit around the straight line and help identify areas of greater uncertainty.

Limitations and future work. The study was conducted at a single site and over a short period, which limits seasonal and spatial generalization; in addition, there may be uncaptured drifts. As a next step, the following are suggested: (i) replicating at multiple sites and seasons, (ii) extending the campaign to capture broad meteorological variability, (iii) comparing with nonlinear models (e.g., random forests, boosting, neural networks) as an additional baseline, and (iv) publishing calibration equations and scripts to promote reproducibility.

REFERENCES

1. Zoran, M. A., Savastru, R. S., Savastru, D. M., Tautan, M. N., Baschir, L. A., Tenciu, D. V. (2022). Assessing the impact of air pollution and climate seasonality on COVID-19 multiwaves in Madrid, Spain. *Environmental Research*, *203*, 111849. https://doi.org/10.1016/j.envres.2021.111849
2. Castell, N., Dauge, F. R., Schneider, P., Vogt, M., Lerner, U., Fishbain, B., … Bartonova, A. (2017). Can commercial low-cost sensor platforms contribute to air quality monitoring and exposure estimates? *Environment International*, *99*, 293–302. https://doi.org/10.1016/j.envint.2016.12.007
3. Karagulian, F., Barbiere, M., Kotsev, A., Spinelle, L., Gerboles, M., Lagler, F., … Borowiak, A. (2019). Review of the performance of low-cost sensors for air quality monitoring. *Atmosphere*, *10*(9), 506. https://doi.org/10.3390/atmos10090506
4. Sharma, V. M., Jain, S. (2025). Unmanned aerial vehicles and low-cost sensors for air quality monitoring: a comprehensive review of applications across diverse emission sources. *Sustainable cities and society*. https://doi.org/10.1016/j.scs.2025.106409
5. Ottosen, T.-B., Ottosen, T.-B., Kumar, P., Kumar, P. (2019). Outlier detection and gap filling methodologies for low-cost air quality measurements. *Environmental Science: Processes & Impacts*, *21*(4), 701–713. https://doi.org/10.1039/c8em00593a
6. Gillooly, S. Gillooly, S., Gillooly, S., Zhou, Y.,… Adamkiewicz, G. (2019). Development of an in-home, real-time air pollutant sensor platform and implications for community use. *Environmental Pollution*, *244*, 440–450. https://doi.org/10.1016/j.envpol.2018.10.064
7. Laura, R., Rojas, N. Y., Nestor, R. (2019). Evaluation of the performance of low-cost sensors as a complement to the Bogotá Air Quality Monitoring Network. *2019 Congreso Colombiano y Conferencia Internacional de Calidad de Aire y Salud Pública (CASP)*. https://doi.org/10.1109/casap48673.2019.9364031
8. Shao, W., Xu, J., Xu, C., Weng, Z., Liu, Q., Zhang, X.,… Gu, A. (2021). Early-life perfluorooctanoic acid exposure induces obesity in male offspring and the intervention role of chlorogenic acid. *Environmental Pollution*, *272*, 115974. https://doi.org/10.1016/j.envpol.2020.115974
9. Chojer, H., Branco, P., Martins, F. G., Sousa, S.I.V. (2024). A novel low-cost sensors system for real-time multipollutant indoor air quality monitoring – development and performance. *Building and Environment*. https://doi.org/10.1016/j.buildenv.2024.112055
10. Morawska, L., Phong, K., Liu, X., Asumadu-Sakyi, A., Ayoko, G., Bartonova, A.,… Williams, R. (2018). Applications of low-cost sensing technologies for air quality monitoring and exposure assessment: How far have they gone? *Environment International*, *116*, 286–299. https://doi.org/10.1016/j.envint.2018.04.018
11. Lewis, A., Edwards, P. (2016). Validate personal air-pollution sensors. *Nature*, (535), 29–31. https://doi.org/10.1038/535029a
12. Chojer, H., Branco, P. T. B. S., Martins, F. G.,

Sousa, S. I. V. (2024). A novel low-cost sensors system for real-time multipollutant indoor air quality monitoring – Development and performance. *Building and Environment*, *266*, 112055. https://doi.org/10.1016/j.buildenv.2024.112055

13. Kelly, K. E., Wei W. Xing, W., Sayahi, T., … Whitaker, R. T. (2020). Community-based measurements reveal unseen differences during air pollution episodes. *Environmental Science & Technology*, *55*(1), 120–128. https://doi.org/10.1021/acs.est.0c02341
14. Wahlborg, D., Björling, M., Mattsson, M. (2021). Evaluation of field calibration methods and performance of AQMesh, a low-cost air quality monitor. *Environmental Monitoring and Assessment*, *193*(5), 251–251. https://doi.org/10.1007/s10661-021-09033-x
15. Badura, M., Batog, P., Drzeniecka-Osiadacz, A., Modzel, P. (2018). Evaluation of low-cost sensors for ambient PM2.5 monitoring. *Journal of Sensors*, *2018*(1), 5096540. https://doi.org/10.1155/2018/5096540
16. Kumar, P., Morawska, L., Martani, C., Biskos, G., Neophytou, M., Di Sabatino, S., … Britter, R. (2015). The rise of low-cost sensing for managing air pollution in cities. *Environment International*, *75*, 199–205. https://doi.org/10.1016/j.envint.2014.11.019
17. Considine, E. M., Reid, C. E., Ogletree, M. R., … Dye, T. (2020). Improving accuracy of air pollution exposure measurements: Statistical correction of a municipal low-cost airborne particulate matter sensor network. *Environmental Pollution*, *268*, 115833–115833. https://doi.org/10.1016/j.envpol.2020.115833
18. Gaury, J., Lafont, U., Bychkov, E., … Biskos, G. (2014). Connectivity enhancement of highly porous WO3 nanostructured thin films by in situ growth of K0.33WO3 nanowires. *CrystEngComm*, *16*(7), 1228–1231. https://doi.org/10.1039/c3ce42078g
19. Peng, J., Hu, M., Wang, Z., … He, L.-Y. (2014). Submicron aerosols at thirteen diversified sites in China: size distribution, new particle formation and corresponding contribution to cloud condensation nuclei production. *Atmospheric Chemistry and Physics*, *14*(18), 10249–10265. https://doi.org/10.5194/acp-14-10249-2014
20. Kumar, P., Morawska, L., Martani, C., … Britter, R. (2015). The rise of low-cost sensing for managing air pollution in cities. *Environment International*, *75*, 199–205. https://doi.org/10.1016/j.envint.2014.11.019
21. Pulster, E. L., Gracia, A., Armenteros, M., Carr, B. E., Mrowicki, J., Murawski, S. A. (2020). Chronic PAH exposures and associated declines in fish health indices observed for ten grouper species in the Gulf of Mexico. *Science of The Total Environment*, *703*, 135551. https://doi.org/10.1016/j.scitotenv.2019.135551
22. Liu, H.-Y., Schneider, P., Haugen, R., … Vogt, M. (2019). Performance assessment of a low-cost PM2.5 Sensor for a near four-month period in Oslo, Norway. *Atmosphere*, *10*(2), 41. https://doi.org/10.3390/atmos10020041
23. Karagulian, F., Barbiere, M., … Borowiak, A. (2019). Review of the performance of low-cost sensors for air quality monitoring. *Atmosphere*, *10*(9), 506. https://doi.org/10.3390/atmos10090506
24. Magoni, M., Rossi, A., Tralli, F., Bernardoni, P., Fabbri, B., Gaiardo, A., … Guidi V. (2024). Novel chemoresistive sensors for indoor CO_2 monitoring: Validation in an operational environment. *ACS Sensors*. https://doi.org/10.1021/acssensors.4c00171
25. Johar, R., Fakieh, E., Allagani, R., Qaisar, S. (2018). A novel and secure smart parking management system (SPMS) based on integration of WSN, RFID, and IoT.
26. Rezapour, A., Tzeng, W.-G., Tzeng, W.-G. (2020). RL-PMAgg: Robust aggregation for PM2.5 using deep RL-based trust management system, *13*, 100347. https://doi.org/10.1016/j.iot.2020.100347
27. Cavaliere, A., Carotenuto, F., Di Gennaro, S. F., … Zaldei, A. (2018). Development of low-cost air quality stations for next generation monitoring networks: calibration and validation of PM 2.5 and PM 10 sensors. *Sensors*, *18*(9), 2843. https://doi.org/10.3390/s18092843
28. Majumdar, D., Purohit, P., Bhanarkar, A.D., Rao, P.S., Rafaj, P., Amann, M., … Srivastava, A. (2020). Managing future air quality in megacities: Emission inventory and scenario analysis for the Kolkata Metropolitan City, India. *Atmospheric Environment*, *222*, 117135. https://doi.org/10.1016/j.atmosenv.2019.117135
29. Wang, F. T., Zhang, K., Xue, J., Xue, J.-F.,… Li, L. (2022). Understanding regional background ozone by multiple methods: a case study in the Shandong Region, China, 2018–2020. *Journal Of Geophysical Research: Atmospheres*, *127*(22). https://doi.org/10.1029/2022jd036809
30. Rong, C., Rong, C., OuYang, S., Sun, H., Sun, H.-J. (2022). Anomaly detection in QAR data using VAE-LSTM with multihead self-attention mechanism. *Mobile Information Systems*, *2022*, 1–14. https://doi.org/10.1155/2022/8378187